BIOCHEMISTRY
including biophysical chemistry & molecular biology
Article

Biochemistry **2011,** *50,* 663–671 663
DOI: 10.1021/bi101523x

Stabilization of the Predominant Disease-Causing Aldolase Variant (A149P) with Zwitterionic Osmolytes[†]

Jack D. Stopa,[‡] Sushil Chandani,[§] and Dean R. Tolan*[,‡,§]

[‡]*Program in Molecular and Cellular Biology and Biochemistry and* [§]*Department of Biology, Boston University, 5 Cummington Street, Boston, Massachusetts 02215, United States*

Received September 19, 2010; Revised Manuscript Received December 15, 2010

ABSTRACT: Hereditary fructose intolerance (HFI) is a disease of carbohydrate metabolism that can result in hyperuricemia, hypoglycemia, liver and kidney failure, coma, and death. Currently, the only treatment for HFI is a strict fructose-free diet. HFI arises from aldolase B deficiency, and the most predominant HFI mutation is an alanine to proline substitution at position 149 (A149P). The resulting aldolase B with the A149P substitution (AP-aldolase) has activity that is <100-fold that of the wild type. The X-ray crystal structure of AP-aldolase at both 4 and 18 °C reveals disordered adjacent loops of the $(\alpha/\beta)_8$ fold centered around the substitution, which leads to a dimeric structure as opposed to the wild-type tetramer. The effects of osmolytes were tested for restoration of structure and function. An initial screen of osmolytes (glycerol, sucrose, polyethylene glycol, 2,4-methylpentanediol, glutamic acid, arginine, glycine, proline, betaine, sarcosine, and trimethylamine *N*-oxide) reveals that glycine, along with similarly structured compounds, betaine and sarcosine, protects AP-aldolase structure and activity from thermal inactivation. The concentration and functional moieties required for thermal protection show a zwitterion requirement. The effects of osmolytes in restoring structure and function of AP-aldolase are described. Testing of zwitterionic osmolytes of increasing size and decreasing fractional polar surface area suggests that osmolyte-mediated AP-aldolase stabilization occurs neither primarily through excluded volume effects nor through transfer free energy effects. These data suggest that AP-aldolase is stabilized by binding to the native structure, and they provide a foundation for developing stabilizing compounds for potential therapeutics for HFI.

Hereditary fructose intolerance (HFI)[1] is an inborn error of metabolism caused by autosomal recessive mutations in the human aldolase B gene (*1*, *2*). Aldolase B is one isozyme of fructose-1,6-bisphosphate aldolase (EC 4.1.2.13), which is found in the liver, kidney, and small intestines (*3*), and the enzyme is crucial for the cleavage of the metabolic intermediate fructose 1-phosphate (Fru 1-P) that yields dihydroxyacetone phosphate (DHAP) and glyceraldehyde in fructose metabolism (*4*). Upon ingestion of fructose, a deficiency in aldolase B activity results in a buildup of Fru 1-P and leads to hypoglycemia, abdominal pain, diarrhea, and vomiting (*2*). Persistent ingestion of the sugar can progress to liver and kidney failure, seizures, growth retardation, coma, and possibly death (*5*). Symptoms are only present upon ingestion of fructose, and currently, the only viable treatment option for HFI is a strict fructose-free diet (*6*). Given the changes in the Western diet (*7*), this is increasingly difficult. Although there are dozens of mutations in *aldoB* known to cause HFI, the most prevalent is a missense mutation resulting in a proline substitution at alanine 149 of aldolase B (A149P). This A149P variant is commonly termed AP-aldolase, and it occurs in approximately 57% of HFI alleles worldwide (*8*).

The AP-aldolase crystal structure shows structural disorder at the site of the A149P substitution that is propagated to adjacent loop regions, including those at one dimer−dimer interface causing a loss of quaternary structure (*9*). This substitution results in a partially active aldolase enzyme that is very sensitive to temperature (*10*). The specific activity toward both cleavage substrates, fructose 1,6-bisphosphate (Fru 1,6-P_2) and Fru 1-P, decreases from 16% of wild-type levels at 10 °C to 0.5% of wild-type levels at 30 °C. The substitution causes a lowered stability of both the secondary (10 °C decrease in $T_{1/2}$) and tertiary (5 °C decrease in $T_{1/2}$) structure of the enzyme. The loss of quaternary structure may be the root of the observed loss of thermal stability and activity, and it agrees with the general thought that the tetrameric structure plays a role in overall protein stability (*11*).

The AP-aldolase offers a potential therapeutic target for HFI given that 82% of HFI patients inherit at least one copy of this allele (*8*). The first question is whether the instability of AP-aldolase can be reversed. In vivo, a class of small organic molecule compounds termed osmolytes are produced to counteract stresses that lead to protein destabilization (*12*). These stresses include osmotic changes, extremes of temperature, high salinity, high pressure, extreme pH, and the presence of protein denaturants such as urea. Osmolytes have been shown to stabilize proteins against all these stresses (*13*−*16*). Concentrations of osmolytes are tightly regulated, through either diet or enzymatic processes, and there are several different osmolytes present in a cell. These

[†]This work was supported in part by National Institutes of Health Grant DK 065089 (to D.R.T.).

*To whom correspondence should be addressed. Phone: (617) 353-5310. Fax: (617) 638-0338. E-mail: tolan@bu.edu.

[1]Abbreviations: AP-aldolase, aldolase B with the Ala-149 to Pro substitution; BSA, bovine serum albumin; CD, circular dichroism; DHAP, dihydroxyacetone phosphate; DTT, dithiothreitol; Fru 1-P, fructose 1-phosphate; Fru 1,6-P_2, fructose 1,6-bisphosphate; G3PDH, α-glycerophosphate dehydrogenase; GAH, glyceraldehyde; GSH, glutathione; HFI, hereditary fructose intolerance; IPTG, β-D-1-thiogalactopyranoside; PBS, phosphate-buffered saline; PEG, polyethylene glycol; TEA, triethanolamine; TIM, triosephosphate isomerase.

Published on Web 12/17/2010

osmolytes generally have low molecular masses and a high solubility in water, in some cases reaching molar concentrations in the cell (*13*, *17*, *18*). Osmolytes can be broken down into three general categories, methylamines, polyols, and certain amino acids (*13*). The current mechanism(s) thought to explain how osmolytes exert their effects on protein structure, which have largely considered reversibly folding proteins, is based on two thermodynamic effects: (i) transfer free energy, through destabilization of the denatured state, and (ii) excluded volume effects (*19*−*23*).

The transfer free energy model for osmolyte-mediated protein stabilization involves an increase in free energy when the protein backbone unfavorably interacts with the osmolyte. This unfavorable interaction destabilizes the denatured state of a protein, shifting the equilibrium of protein folding toward the native state in the presence of protecting osmolytes (*21*). On the other hand, in the presence of protein denaturants, such as urea or guanidine (deprotecting osmolytes), the denatured state is stabilized. In this model, the presence of protecting osmolytes results in unfavorable interactions of the solvent with the protein backbone (*19*, *21*); thus, the overly exposed protein backbone in the denatured state is destabilized relative to the folded protein.

The excluded volume model for osmolyte-mediated protein stabilization is an indirect effect. The model considers the volume occupied by the high concentration of osmolyte in solution, which results in a crowded environment (*22*). In this environment, a macromolecule will favor the folded state, which has a smaller volume than the denatured state (*24*). According to this model, the larger the osmolyte molecule, the greater the occupied volume; therefore, the native state would be more favored in solution (*23*, *25*).

This study investigated whether a small molecule could counteract the temperature-dependent instability caused by the A149P substitution. After a screen of osmolytes in the three general categories, zwitterionic compounds, in particular the amino acid glycine, fully restored the secondary and tertiary structure stability of AP-aldolase to wild-type melting temperatures, staving off the start of the irreversible unfolding reaction. In addition, glycine stabilized the aldolase tetrameric quaternary structure and increased activity more than 10-fold, to ~4% of that of the wild type. Different sized zwitterionic osmolytes with different fractional polar surface areas (FPSA) were tested, and the results indicated that the mechanisms of osmolyte-mediated stabilization for reversibly folding proteins do not completely explain the data for AP-aldolase. These results could potentially lead to further improvement in the stabilization of AP-aldolase by its interaction of small molecules.

EXPERIMENTAL PROCEDURES

Materials. The enzymes α-glycerophosphate dehydrogenase (G3PDH), triosephosphate isomerase (TIM), lysozyme, and thrombin were from Sigma (St. Louis, MO). Plasmid pGEX-2T, molecular mass standards, and glutathione Sepharose 4B were purchased from GE Healthcare Life Sciences. Bacto yeast extract and tryptone peptone were purchased from VWR. Triton X-100 was obtained from Eastman Kodak (Rochester, NY). Fru 1,6-P_2, Fru 1-P, isopropyl β-D-1-thiogalactopyranoside (IPTG), glutathione (GSH), and other chemicals were from Sigma.

Expression and Purification of Recombinant Aldolase B and AP-Aldolase. Wild-type aldolase B and AP-aldolase were produced by heterologous expression in *Escherichia coli* DH5α as previously described (*10*). AP-aldolase was purified as a glutathione *S*-transferase fusion protein and subsequently cleaved by thrombin, and elution in 137 mM NaCl, 2.7 mM KCl, and 12 mM phosphate (pH 7.4) (PBS) yielded the full-length protein (*10*). Aldolase B was purified by affinity elution ion-exchange chromatography as previously described (*26*). Both enzymes were stored in 70% saturated ammonium sulfate at 4 °C.

Determination of Protein Concentration. Protein concentrations were determined by dye binding (*27*) using bovine serum albumin (BSA) as a standard or by absorbance at 280 nm ($E_{280}^{0.1\%} = 0.85\ M^{-1}\ cm^{-1}$) (*28*).

Circular Dichroism Spectrophotometry. The far-UV CD spectra (185−250 nm) were recorded at 4 °C using the Aviv 62DS spectrometer with a 0.1 mm path length quartz cuvette. Data were collected in 1 nm increments with a 15 s averaging time. The effect of temperature on protein secondary structure was monitored at 222 nm in 2 °C increments (30 s equilibration time) from 10 to 80 °C, with a 15 s averaging time. The protein concentration was 1.0 mg/mL in PBS containing 0.5 mM DTT. Near-UV CD spectra (250−320 nm) were recorded similarly in a 1 mm path length quartz cuvette. The temperature dependence of the ellipticity at 263 nm was monitored in 2 °C increments from 20 to 70 °C, with a 15 s averaging time.

Gel Filtration Chromatography. Prior to the experiment, purified aldolase in ammonium sulfate was dialyzed twice at 4 °C against approximately 2500 volumes of PBS containing 0.5 mM DTT. Protein samples were loaded onto a Superdex-200 FPLC column (Pharmacia) at 4 °C. The absorbance of the eluate at 0.5 mL/min was monitored at 280 nm. The molecular masses of the eluting species were calculated from a standard curve consisting of thyroglobulin (669 kDa), ferritin (440 kDa), aldolase (159 kDa), conalbumin (75 kDa), and ovalbumin (43 kDa).

Aldolase Activity. Aldolase cleavage kinetics toward Fru 1,6-P_2 and Fru 1-P were measured in coupled assays containing NADH, G3PDH, and TIM, as previously described (*29*, *30*).

Thermal Inactivation. The effect of an osmolyte on thermal inactivation of aldolase activity was monitored by first diluting the enzyme to 0.4 mg/mL with the desired concentration of osmolyte in 50 mM triethanolamine (TEA) (pH 7.4). An aliquot was assayed for Fru 1,6-P_2 cleavage activity prior to thermal incubation. The enzyme/osmolyte solution was then incubated at 30 °C for 5 min and then at 10 °C for 2 min. The solution was centrifuged at 25 °C and 2000*g* for 1 min to remove any aggregated material. Another aliquot was assayed for Fru 1,6-P_2 cleavage activity at 25 °C to measure the protection from thermal inactivation. All activity values were normalized to a no osmolyte preincubation activity.

Molecular Dynamics. Molecular construction and manipulations were conducted using the InsightII and Discovery suites from Accelrys Inc. Simulations were performed using the CHARMm force field (release 30) (*31*) on an IBM p655 computer. The molecular series from 2-aminoacetic acid to 7-aminoheptanoic acid was built ab initio, the total charge set to zero, and the series optimized. A short, 50 ps molecular dynamics run in vacuo yielded compact conformers, in the cis orientation for the longer chains. These were soaked in ~1200 molecules of water, and dynamics was continued for 3 ns. In the case of 6-aminohexanoic acid and 7-aminoheptanoic acid, the backbone dihedrals were then rotated to the trans orientation, and an ensemble of seven randomly placed copies each of the cis and trans forms, in ~1200 molecules of water. The molecular volume, radius of gyration, and surface area were calculated as defined by InsightII and Discovery suites using the equations of Stanton and Jurs (*32*). The relative hydrophobic surface area (RHSA) and the FPSA

Table 1: Screen of Potential Stabilizing Osmolytes

class	osmolyte	concn	specific activity (%)[a] preincubation	postincubation
controls	none	−	100 ± 12	20 ± 7
	urea	1 M	38 ± 8.7	7 ± 0.22
polyols	glycerol	4 M	126 ± 42	52 ± 3.8
	2,4-methylpentanediol (MPD)	4 M	10 ± 1.0	17 ± 0.87
	PEG-8000	2% (w/v)	126 ± 10	27 ± 0.30
	sucrose	1 M	124 ± 10	42 ± 0.95
methylamines	trimethylamine *N*-oxide (TMAO)	1 M	66 ± 5.6	43 ± 2.5
	betaine	4 M	103 ± 9.3	101 ± 10
	sarcosine	1 M	106 ± 18	98 ± 10
amino acids	glycine	2 M	138 ± 10	127 ± 18
	arginine	1 M	6 ± 0.45	1 ± 0.35
	proline	3 M	122 ± 14	35 ± 0.38

[a]Calculated using the enzyme-coupled aldolase activity assay and normalizing to preincubation without osmolyte. (100% = 0.02 unit/mg).

were measured on 140 structures selected from 10 equally spaced intervals from the last 1 ns of the simulations.

RESULTS

Osmolyte Screening. Measuring enzymatic activity as a function of temperature provides a very sensitive way to appraise the effects of a potential stabilizing osmolyte on an enzyme and allows quantification of perturbations in protein structure. A thermal inactivation assay was developed for potential stabilizing osmolytes on the HFI-causing AP-aldolase enzyme. AP-aldolase has maximal activity at < 15 °C but gradually loses activity at increasing temperatures, having negligible activity at 37 °C (200-fold lower than that of the wild type) (*10*). For the initial screen of osmolytes, an inactivating temperature of 30 °C was chosen. Five minutes at 30 °C results in an 80% loss of AP-aldolase activity. Several osmolytes from each osmolyte class (methylamines, polyols, and amino acids) were tested using concentrations that have been effective for other proteins (*33*). AP-aldolase was diluted to 0.4 mg/mL in TEA buffer containing each osmolyte and subjected to the thermal inactivation assay. The preincubation assay served to control for any non-temperature-dependent effects on AP-aldolase. In addition, a negative control of AP-aldolase in 1 M urea yielded a decreased but still measurable amount of activity after incubation. The results of this initial screen are listed in Table 1. All pre- and postincubation values were normalized to the preincubation assay without osmolyte. The osmolytes most effective at stabilizing AP-aldolase activity at 30 °C were betaine, sarcosine, and glycine.

Optimal Osmolyte Concentration Determination. The optimal concentration of glycine necessary for stabilizing AP-aldolase in the thermal inactivation assay was determined by testing concentrations of glycine between 0.125 and 2.0 M. Below 2 M glycine, the complete stabilization effect on AP-aldolase was essentially lost, although at 1 and 0.5 M some significant protection against thermal inactivation remained (Figure 1). At 0.25 M glycine, the protective effect on thermal inactivation was lost. Glycine must be present at concentrations of 2 M to fully stabilize AP-aldolase activity at 30 °C in vitro.

Determination of the Osmolyte Functional Moiety Necessary for Stabilization. The three most effective osmolytes were glycine, sarcosine, and betaine. These three osmolytes are structurally related, each being zwitterionic at physiological pH and differing as primary, secondary, and quaternary amines, respectively.

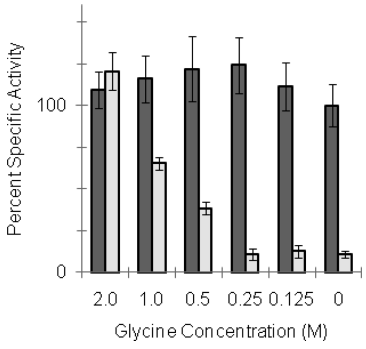

FIGURE 1: Two molar glycine is necessary for the desired effect on the stability of AP-aldolase. Thermal inactivation assays at 30 °C were performed on AP-aldolase (0.4 mg/mL) in the presence of glycine at concentrations varying from 0 to 2 M. Preincubation (dark) and postincubation (light) activity values are normalized to the preincubation, no-compound control value (~0.01 unit/mg). All trials were performed at pH 7.4. Error bars are presented as 1σ of three separate trials.

Exploration of the structural element(s) important for stabilizing AP-aldolase used a group of molecules that separated the structural element(s) of these osmolytes. Alanine, β-alanine, ethanolamine, ethylamine, propionic acid, and acetic acid were used in the thermal inactivation assay (Table 2). Alanine and β-alanine, an alanine isomer, were closely related in size and structure to glycine. Both ethylamine and ethanolamine maintained a positively charged amino group at pH 7.4 but lacked the negatively charged carboxyl group, although ethanolamine maintained a polar end. Propionic acid and acetic acid were used to probe the role of the carboxyl group alone. Lastly, equal amounts of triethylamine and acetic acid were tested, thus separating the charges completely. Compounds other than the amino acids, including the triethylamine/acetic acid mixture did not result in any thermal protection and destroyed enzyme activity. Thermal inactivation assays using these compounds showed that both charges were necessary on the same molecule for stabilizing AP-aldolase (Table 2).

Analyzing the Effects of Glycine on Secondary and Tertiary Structure. The effects of glycine on the perturbed secondary and tertiary structures of AP-aldolase were investigated by CD spectrophotometry. A melting curve was generated by monitoring the CD absorbance of AP-aldolase at 222 nm from 10 to 80 °C (Figure 2). In the presence of glycine, AP-aldolase

Table 2: Screen of Functional Groups Required for Stabilizing AP-Aldolase Activity

		SPECIFIC ACTIVITY (%)[a]	
COMPOUND[b]	STRUCTURE	PRE-INCUBATION	POST-INCUBATION
Alanine	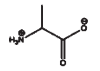	110 ± 28	160 ± 17
β-alanine	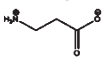	100 ± 17	110 ± 29
Ethanolamine	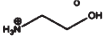	22 ± 10	19 ± 19
Ethylamine		21 ± 8	23 ± 15
Propionic Acid	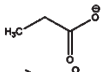	82 ± 13	21 ± 5
Acetic Acid		16 ± 9	16 ± 5
Triethylamine + Acetic Acid		12 ± 3	18 ± 2

[a]Calculated using the enzyme-coupled aldolase activity assay and normalizing to preincubation without osmolyte (100% = 0.03 unit/mg). [b]All at 2 M.

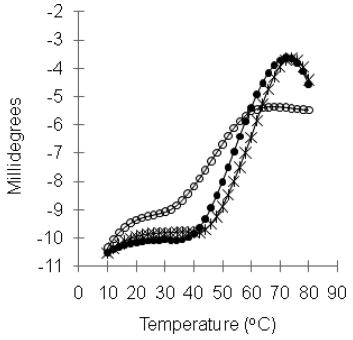

FIGURE 2: Secondary structure of AP-aldolase stabilized in the presence of 2 M glycine. Far-UV CD measurements were taken from 10 to 90 °C in 2 °C increments at 222 nm at a concentration of 1.0 mg/mL AP-aldolase in the presence (●) and absence (○) of 2 M glycine. Wild-type aldolase B in the absence of glycine was subjected to the same conditions, and the results are shown for comparison (×).

exhibited a melting curve similar to that of wild-type aldolase B. The presence of glycine shifted the $T_{1/2}$ from 45 to ~55 °C, ~3 °C lower than that of wild-type aldolase B. The overall secondary structure of AP-aldolase was not greatly affected by the A149P substitution when compared to the overall secondary structure of the wild-type protein (*10*), and the presence of glycine did not change the far-UV spectrum of AP-aldolase (data not shown).

The near-UV CD spectrophotometric spectra of AP-aldolase and wild-type aldolase B were different, and the presence of glycine could not change the AP-aldolase spectrum to resemble that of wild-type aldolase B at 10 °C (Figure 3A). However, much like the secondary structure, the tertiary structure of AP-aldolase was sensitive to temperature (*10*). CD spectrophotometry examined the effect of glycine on changes in the near-UV CD absorbance for AP-aldolase as a function of temperature at 263 nm from 10 to 70 °C (Figure 3B). In the presence of glycine, the melting curve of AP-aldolase resembled that of the wild type. AP-aldolase in the absence of glycine had a $T_{1/2}$ of 44 °C, in contrast to the $T_{1/2}$ of the wild-type protein and AP-aldolase in the presence of glycine, which was 53 °C. This indicated that, although overall differences in AP-aldolase tertiary structure remained, glycine was able to restore the stability of the tertiary structure.

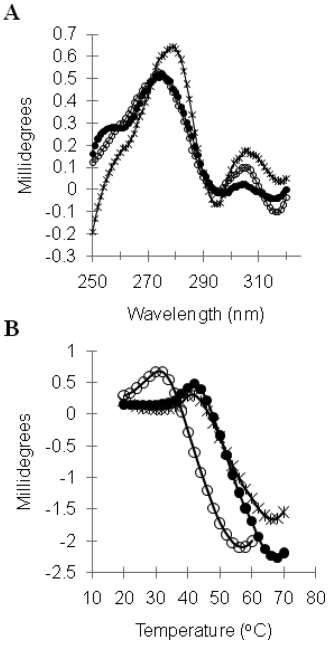

FIGURE 3: Tertiary structure of AP-aldolase stabilized in the presence of 2 M glycine. (A) Near-UV CD spectra were collected at 250−320 nm in a 0.1 cm path length quartz cuvette at an AP-aldolase concentration of 1.0 mg/mL at 10 °C in the presence (●) and absence (○) of 2 M glycine. Wild-type aldolase B in the absence of glycine was subjected to the same conditions, and the results are shown for comparison (×). Data were collected in 1 nm increments with a 10 s averaging time. (B) Near-UV CD measurements were taken from 10 to 90 °C in 2 °C increments at 263 nm at an AP-aldolase concentration of 1.0 mg/mL in the presence (●) and absence (○) of 2 M glycine. Wild-type aldolase B in the absence of glycine was subjected to the same conditions, and the results are shown for comparison (×).

Effect of Glycine on Quaternary Structure. The disorder of several loops in AP-aldolase at the dimer−dimer interface perturbed the aldolase B dimer ↔ tetramer equilibrium (*9*, *10*). The loss of quaternary structure in aldolases is highly correlated with the loss of thermal stability (*11*, *34*). The question of whether the thermal stabilization afforded by glycine correlates with an increased level of quaternary structure of AP-aldolase arises.

Changes in quaternary structure with and without glycine were determined by size-exclusion chromatography. In the absence of glycine at 4 °C, the dominant species of AP-aldolase in solution was the dimeric (> 2-fold over the tetramer) and wild-type aldolase B was tetrameric, which has been previously reported (*3*, *10*) (Figure 4A). In the presence of glycine at 4 °C, the dominant species was tetrameric (Figure 4B). The correlation of regained tetrameric structure with thermal stability of the secondary and tertiary structure and the activity could be the basis for the effects of glycine on AP-aldolase.

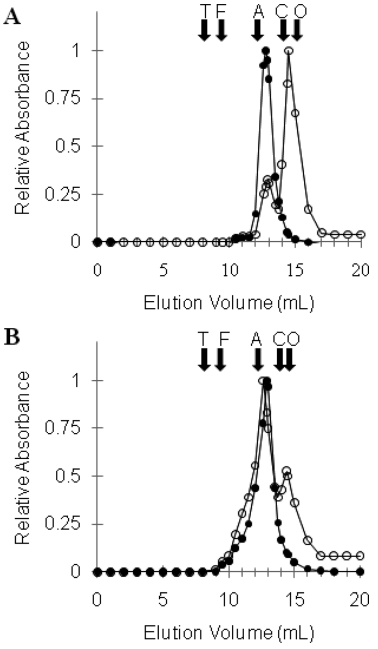

FIGURE 4: Quaternary structure of AP-aldolase stabilized in the presence of 2 M glycine. Gel filtration was performed on AP-aldolase (○) and aldolase B (●) at a concentration of 8 mg/mL using a Superdex-200 column in the absence (A) and presence (B) of 2 M glycine at 4 °C. Results are normalized to the peak fraction; 1 is set equal to 1.8 absorbance units at 280 nm. Arrows indicate the peak of elution for markers: T, thyroglobulin; F, ferritin; A, aldolase A; C, conalbumin; O, ovalbumin.

Effect of Glycine on Enzymatic Activity and Substrate Affinity. In addition to the A149P substitution perturbing the dimer−dimer interface, the active site is disturbed, which results in a 20-fold increase in the K_m value toward Fru 1-P (*10*). Should the increased structural stability observed in the presence of glycine result in the re-formation of quaternary structure alone, a restoration of K_m values in the presence of glycine would not necessarily follow. Because of its instability and to ensure maximal retention of activity during purification, AP-aldolase was purified in the presence of 2 M glycine starting from cell lysis. The steady-state kinetic constants of AP-aldolase toward substrates Fru 1,6-P_2 (Table 3) and Fru 1-P (Table 4) were examined at 10 and 30 °C in the presence and absence of 2 M glycine.

At 10 °C, the effect of glycine on k_{cat} values toward Fru 1,6-P_2 was insignificant; however, at 30 °C, the presence of glycine resulted in a 10−13-fold improvement in activity when compared to that of the enzyme in the absence of glycine. The unchanged value of k_{cat} for AP-aldolase at 10 °C with or without glycine indicated that at 10 °C AP-aldolase is at its most stable structure. In the presence of glycine, the K_m value toward Fru 1,6-P_2 at 10 °C unexpectedly increased when compared to the value in the absence of glycine, but this effect decreased at 30 °C.

A more striking improvement in the K_m value was found with Fru 1-P for AP-aldolase in the presence of glycine (Table 4). At both temperatures, the K_m values in the presence of glycine were within 1.6−3-fold of that of the wild type. This was a vast improvement compared with AP-aldolase in the absence of glycine, whose K_m values were approximately 20-fold greater than that of the wild type. The k_{cat} values toward Fru 1-P were affected by glycine like those toward Fru 1,6-P_2; a larger effect was seen at 30 °C than at 10 °C, although it is notable that at 10 °C the activity of AP-aldolase toward Fru 1-P was within 30% of that of the wild type. These results suggested that, although the AP-aldolase active site remained slightly different from that of the wild type, the presence of 2 M glycine improved the catalytic efficiency (k_{cat}/K_m) toward Fru 1-P by more than 150-fold at 30 °C. Lastly, the changes in K_m values toward either substrate indicated that the effects of glycine at the active site might be unrelated to the effect of glycine on restoring quaternary or tertiary structural stability.

Table 3: Effect of 2 M Glycine on Kinetic Values of AP-Aldolase at 10 and 30 °C with the Substrate Fructose 1,6-Bisphosphate

	10 °C				30 °C			
enzyme	k_{cat} (s^{-1})	%[a]	K_m (μM)	ratio[b]	k_{cat} (s^{-1})	%[a]	K_m (μM)	ratio[b]
aldolase B[c]	0.190 ± 0.002	−	1.7 ± 0.2	−	2.1 ± 0.02	−	2.4 ± 0.4	−
AP-aldolase	0.029 ± 0.006	15	2.8 ± 0.3	1.6	0.008 ± 0.00002	0.38	15.9 ± 0.01	6.6
AP-aldolase+glycine	0.028 ± 0.002	15	33 ± 4.0	20	0.076 ± 0.012	3.7	27.9 ± 5.6	12

[a]Measured as a percentage of wild-type activity. [b]Measured as a ratio with the K_m value of wild-type aldolase. [c]Values reported in ref *10*.

Table 4: Effect of 2 M Glycine on Kinetic Values of AP-Aldolase at 10 and 30 °C with the Substrate Fructose 1-Phosphate

	10 °C				30 °C			
enzyme	k_{cat} (s^{-1})	%[a]	K_m (μM)	ratio[b]	k_{cat} (s^{-1})	%[a]	K_m (μM)	ratio[b]
aldolase B[c]	0.120 ± 0.004	−	240 ± 10	−	2.0 ± 0.2	−	880 ± 80	−
AP-aldolase[c]	0.019 ± 0.006	16	4200 ± 460	20	0.008 ± 0.00004	0.4	16400 ± 980	20
AP-aldolase+glycine	0.035 ± 0.002	30	640 ± 95	2.7	0.152 ± 0.005	8	2190 ± 290	2.5

[a]Measured as a percentage of wild-type activity. [b]Measured as a ratio with the K_m value of wild-type aldolase. [c]Values reported in ref *10*.

Determination of the Optimal Size of the Zwitterionic Osmolyte. Much insight into the mechanism of osmolyte action has been gained, largely using small monomeric two-state folding proteins. Two major theories often used to explain these stabilizing effects are excluded volume and transfer free energy (*20*). According to the excluded volume theory, larger osmolytes should strengthen any stabilizing effects, whereas according to the transfer free energy theory, a decrease in FPSA should strengthen any stabilization effects. Further exploration of the stabilization of AP-aldolase was tested with zwitterions of different sizes and different FPSAs (Figure 5A). The different sized zwitterions had increasing numbers of methylene groups between the amino and carboxylate groups. Increasing the size of the osmolyte produced no significant increase in the level of protection against thermal inactivation. As size increased, however, the larger zwitterions lost their effect. The γ-aminobutyric acid with three methylene groups was just as effective as glycine and β-alanine, but δ-aminopentanoic acid was able to protect the enzyme only ~50% and ε-aminohexanoic acid only ~20%. For the case of 7-aminoheptanoic acid, the compound inhibited activity altogether. These data revealed that both positive and negative functional groups in a single molecule were required for effective stabilization of AP-aldolase, and that the zwitterion must be of a certain size.

The molecular volume, radius of gyration, solvent-accessible surface area, FPSA, and relative hydrophobic surface area (RHSA) were calculated from structures of these compounds after molecular dynamics simulations for 3 ns. There was a linear increase in molecular volume that demonstrated a 2-fold increase from glycine to ε-aminohexanate (data not shown). The larger osmolytes in this linear range were accompanied by a decrease in thermal stabilization rather than an increase, which excluded volume theory would predict. The radius of gyration, solvent-accessible surface area, and RHSA were not linearly increasing after δ-aminopentanoic acid, and there was a striking correlation of RHSA with the loss of stabilization (Figure 5B). As the size of the molecules increased, there was a linear increase in RHSA until δ-aminopentanoic acid, the first compound unable to fully protect AP-aldolase from thermal inactivation (Figure 5A). The average structures after molecular dynamics simulation showed a tendency to be more compacted as the charged groups tended to interact intramolecularly (Figure 5C). The largest compound, 7-aminoheptanoic acid, showed a detergent-like structure that perhaps explained its non-temperature-dependent inhibition of activity.

According to the transfer free energy model, increased osmolyte-induced stabilization of reversibly folding proteins correlates with a decreased FPSA (*19*). The FPSA of these zwitterions was calculated and plotted versus their observed percentage protection of AP-aldolase from thermal inactivation (Figure 5D). What was observed was the opposite correlation. Increased osmolyte-induced stabilization of AP-aldolase correlated with increased FPSA, with perhaps the exception of GABA.

The lack of correlation of stability with decreasing FPSA and increasing size of the osmolyte suggests that neither the free energy transfer nor the excluded volume model explains the mechanism of osmolyte-mediated protein stabilization of AP-aldolase. Another model is one in which the osmolytes interact with and stabilize the native state of the protein. Consistent with this model, the concentration dependence of glycine versus an indirect result of any binding, protection of AP-aldolase from thermal inactivation, was measured between 0 and 3 M. The data fit well to a sigmoidal binding curve (Figure 6A) with the best fit to such a curve (R^2 = 0.99) showing saturation at ~30 M (Figure 6B), which is well beyond the 3.3 M solubility of glycine. The apparent K_d was 6.6 ± 0.4 M, and the Hill plot gave a coefficient of 2.06 ± 0.11. Clearly, this theoretical binding has a very low affinity with multiple sites. These data suggest that glycine has binding sites that can stabilize AP-aldolase to thermal inactivation, and they may offer another explanation for osmolyte-mediated protein stability in general.

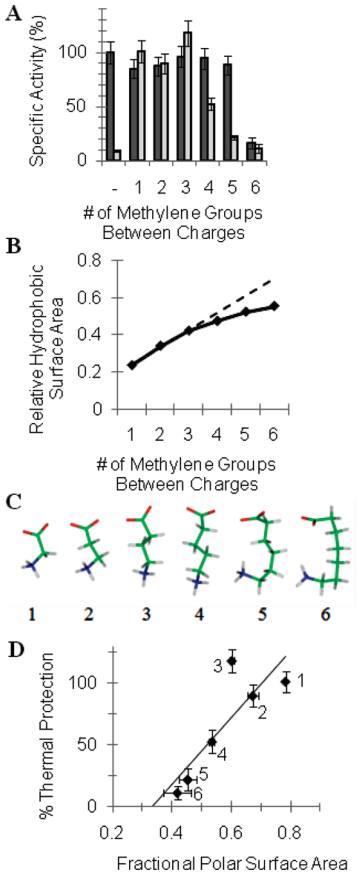

FIGURE 5: Size of the zwitterionic osmolyte is crucial for stabilizing AP-aldolase. (A) Thermal inactivation assays at 30 °C were performed on AP-aldolase (0.4 mg/mL) in various compounds at 2 M with an increasing number of methylene groups between charged ends indicated at the bottom. Preincubation (dark) and postincubation (light) activity values are normalized to the preincubation, no-compound control value (0.07 unit/mg). All trials were performed at pH 7.4. Error bars are presented as 1σ of three separate trials. Reagents were as follows: 1, glycine; 2, β-alanine; 3, γ-aminobutryic acid (GABA); 4, δ-aminopentanoic acid (DAPA); 5, ε-aminohexanoic acid (EAHA); 6, 7-aminoheptanoic acid (7AHA). (B) Average RHSA calculated from molecular dynamics simulations of the molecular series of compounds plotted vs the number of methylene groups between charged ends. The RHSA was calculated from structures obtained in the molecular dynamics simulations by first summing the solvent-accessible surface areas of atoms with an absolute partial charge of < 0.2 and termed the total hydrophobic surface area (THSA). This was divided by the molecular solvent accessible surface area (SASA), which was calculated with the solvent represented as a probe with a radius of 1.4 Å. Partial charge assignments were made in the CHARMm force field and hydrophobic atoms defined as having a partial charge of < 0.2. (C) Representative structures of the molecular series, chosen for RHSA values that approach the average values depicted in panel B. (D) FPSA plotted vs the percent thermal inactivation protection observed from panel A. The linear regression line (—) has a positive slope with a correlation coefficient of 0.72. The FPSA was calculated from structures obtained in the molecular dynamics simulations as described for panel B using the sum of surface areas of atoms with an absolute value of partial charges of ≥ 0.2, termed the total polar surface area (TPSA), and divided by SASA.

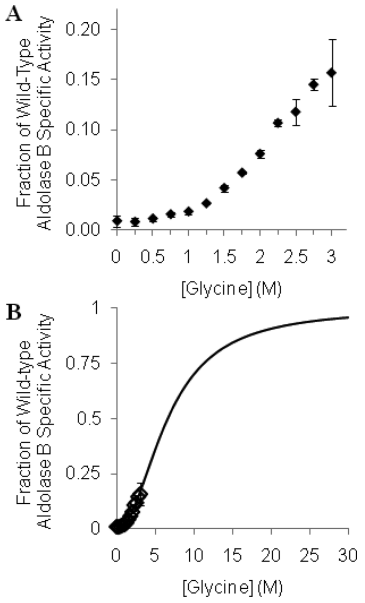

FIGURE 6: Glycine concentration vs thermal stabilization fits a sigmoidal binding curve. (A) Thermal inactivation assays were performed at 30 °C on AP-aldolase (0.5 mg/mL) in the presence of glycine at concentrations varying from 0 to 3 M. Values of residual specific activity of AP-aldolase were normalized to that of wild-type aldolase B at 25 °C (1 unit/mg). All trials were performed at pH 7.4. Error bars are presented as 3σ of three separate trials. (B) Same data in panel A fit to a sigmoidal binding curve with the equation $Y = [S]^n/(K_d' + [S]^n)$ using KaleidaGraph (Synergy Software) ($R^2 = 0.9890$).

DISCUSSION

Effects of the A149P Substitution on Aldolase Structure and Activity. Previous reports about AP-aldolase have hypothesized that the structural perturbation at Pro-149 causes two separate and perhaps unrelated problems, one affecting structural stability and temperature sensitivity through the loss of quaternary structure and another affecting the maximal activity of the enzyme by perturbations at the active site (*9*, *10*). This idea arose from the observation that the loss of activity of AP-aldolase occurs well before any detectable loss of secondary or tertiary structure. Consistent with this, the crystal structure of AP-aldolase shows that Arg-148, which typically forms a salt bridge with Glu-189 (forming a wall of the active site cleft), was in a salt bridge with Glu-187, a critical residue involved in acid−base catalysis (*35*), thus potentially altering the electrostatics at the active site (*9*). In addition, the nearby essential catalytic residue Lys-146 (*36*) had a slightly altered orientation because of the substitution of the adjacent proline. Finally, Arg-303, a well-known C1-phosphate binding site (*37*), was not in the wild-type conformation, which could explain the large increases in K_m values toward Fru 1-P at both 10 and 30 °C (*10*). Concentrations of glycine of 2 M completely restored wild-type stability in the secondary and tertiary structure of AP-aldolase and, furthermore, stabilized the wild-type tetrameric structure, although not to full wild-type levels. In addition to this structural stabilization, glycine restored activity toward Fru 1-P to 30% of that of the wild type. Although AP-aldolase did not regain wild-type activity in the presence of glycine compared to that in the absence of glycine, there was a >10-fold improvement in the degree of activity retained at 30 °C. That glycine had increased both structural stability and activity indicated that the two problems with AP-aldolase might be intertwined. Similar losses of enzyme activity without observable structural changes have been reported for other enzymes (*38*, *39*), and it would be interesting if glycine had similar effects.

Mechanism of Osmolyte-Mediated Protein Stabilization. In other studies of osmolyte action, excluded volume effects have been shown to play a major role (*20*, *40*). For example, using various osmolytes of the polyol class of increasing size ranging from glycerol to the trisaccharide melezitose to study the folding of yeast iso-1-ferricytochrome *c*, a correlation between an increase in protein stability and osmolyte size was found (*23*). This correlation strongly supported the excluded volume model of osmolyte-mediated protein stabilization for this reversibly folding protein.

The transfer free energy model focuses on the thermodynamic interaction between a reversibly folding protein and solvent, either with or without osmolyte. Numerous studies have shown that osmolytes affect interactions between the protein backbone (as opposed to the R groups) and solvent (*41*−*44*). The protein backbone, which needs to be highly solvated for a protein to be fully denatured, has an unfavorable interaction with osmolyte-containing solutions. This osmolyte−backbone interaction has a much higher transfer free energy than the water−backbone interaction. So, when the transition from water as the solvent to a solution with a high concentration of osmolyte is made, the free energy of the denatured state increases, thus shifting the folding equilibria in favor of the native state. Furthermore, it has been shown that this transfer free energy, when used as a measure of osmolyte-mediated protein stabilization, correlates with an individual osmolyte's relatively smaller FPSA. This specific characteristic of an osmolyte molecule might be the source of its ability to stabilize protein structure (*19*). Although the mechanism of osmolyte action for most proteins remains unclear, major contributions involving both these effects are likely involved (*20*).

In this study, charged zwitterionic osmolytes were important in the osmolyte-mediated stabilization of AP-aldolase. If glycine were acting via the transfer free energy model, the polarity of these molecules would play a crucial role in the stabilizing effects toward AP-aldolase. Consistent with this, smaller methylamine osmolytes, such as betaine and sarcosine, have smaller FPSA values compared to polyol osmolytes such as sucrose and glycerol, and these smaller osmolytes had an increased capacity for stabilization of AP-aldolase (Table 1). On the other hand, if a relatively low FPSA were crucial for the osmolyte-mediated stabilization of AP-aldolase, which has been predicted computationally for similar compounds (*19*), then increasing the size of the zwitterion without adding any further polarity should lower the FPSA and further stabilize AP-aldolase. This was not observed, and in fact, the opposite correlation was observed (Figure 5D). Furthermore, it was not simply the charges of the osmolyte that were required; these charges were required to be on the same molecule and not too distant from each other. Were the charges all that were necessary, then equal amounts of positively and negatively charged compounds would have stabilized AP-aldolase as well as glycine, which was not the case. Perhaps if the overall polarity were maintained with the larger zwitterions, their effectiveness in stabilizing AP-aldolase would increase and include favorable excluded volume effects, as seen with larger osmolytes such as sucrose (*23*).

Were the excluded volume model of osmolyte action be the major driving force for the stabilization effects on AP-aldolase, then simply increasing the size of the zwitterion would decrease the available volume and force the N ↔ D equilibrium toward the N state, which has a smaller radius. This was not observed. Taken

together, these results do not support a model in which these small zwitterionic osmolytes stabilize AP-aldolase through either a transfer free energy or an excluded volume mechanism, although it is possible that excluded volume plays a minor role in stabilizing AP-aldolase in response to temperature [GABA seemed to increase the stabilization slightly over the smaller β-alanine (Figure 5A)]. There are at least two very complex reactions at play here, namely, relative reaction rates of folding intermediates and the differential interactions of these intermediates with the osmolytes; however, this lack of consistency with these models of osmolyte action indicated another mode of action. It is possible that these zwitterionic osmolytes are directly interacting with the native state of the protein, forcing the protein to adopt a more stable conformation than in a solution without osmolyte present. Several of these osmolytes increased enzyme activity before any thermal inactivation (see the 10 °C data in Tables 1 and 2), indicating a stabilizing effect before significant denaturation. Moreover, unlike most of the reversibly folding proteins used for testing models of osmolyte action, AP-aldolase is not able to reversibly unfold in the assay used here. In particular, the transfer free energy model is based on the osmolyte's ability to shift the equilibrium between the native and denatured states, and if there is no equilibrium or it is largely perturbed by aggregation, then these models would not readily apply. The thermal melting of AP-aldolase is not reversible above 20 °C (*45*). Given that the thermal stabilization assays was performed at 30 °C, AP-aldolase was not in equilibrium with its unfolded state, which was largely precluded by irreversible aggregation. Furthermore, the effects of glycine on AP-aldolase activity showed that during the 5 min incubation at 30 °C there was no change in secondary or tertiary structure as determined by CD (Figures 2 and 3), thus indicating little change in the N ↔ D equilibrium, although parts of the protein, such as loops that are invisible to CD spectroscopy, could be in such a reversible transition. Overall, these observations of increased activity and stability of AP-aldolase at temperatures lower than those needed for significant structural perturbation suggest that the osmolyte-mediated protein stabilization of AP-aldolase is most likely affecting the native state of the protein, although the possible involvement of osmolyte-affected transfer free energy on partially denatured structures and minor excluded volume effects cannot be ruled out. Consistent with this model for direct binding of osmolytes to the native structure, such binding was observed for proline to an allosteric site on pyruvate kinase (*46*).

Using Small Molecules as a Treatment for HFI. Currently, the only viable treatment option for patients afflicted with HFI is complete avoidance of fructose in their diets. The discovery herein of zwitterions useful in stabilizing AP-aldolase leads to the prospect of designing small molecules that could potentially lead to treatments. Most rational drug designs are for inhibitors, as opposed to compounds that stabilize proteins and allow for natural function. An intelligently designed drug, taking into account the observed effect of zwitterionic molecules on AP-aldolase, and using a molecule with a structure similar to that of glycine as a starting point, would only need to produce an additional 10-fold increase in activity to restore AP-aldolase to near wild-type activity. Thus, the idea that a small molecule can enforce the structural stability of AP-aldolase at 37 °C and be useful as a therapeutic for HFI may have merit. Further studies aim to examine any potential binding sites of glycine on aldolase, which may provide a potential stabilizing binding pocket, and would be useful in the intelligent design of a zwitterionic compound with increased affinity for the surface of AP-aldolase.

ACKNOWLEDGMENT

We thank Drs. Gary Jacobson and Mary Roberts for critical reading of the manuscript.

REFERENCES

1. Hers, H.-G., and Joassin, G. (1961) Anomalie de l'aldolase hepatique dans l'intolerance au fructose. *Enzymol. Biol. Clin. 1*, 4–14.
2. Steinmann, B., Gitzelmann, R., and Van den Berghe, G. (2001) Disorders of Fructose Metabolism. In The Metabolic and Molecular Basis of Inherited Disease (Scriver, C., Beaudet, A., Sly, W., and Valle, D., Eds.) pp 1489−1520, McGraw-Hill, Inc., New York.
3. Lebherz, H. G., and Rutter, W. J. (1969) Distribution of fructose diphosphate aldolase variants in biological systems. *Biochemistry 8*, 109–121.
4. Hers, H., and Kusaka, T. (1953) Le Métabolisme du fructose 1-phosphate dans le foie. *Biochim. Biophys. Acta 11*, 427–432.
5. Cox, T. M. (1993) Iatrogenic deaths in hereditary fructose intolerance. *Arch. Dis. Child. 69*, 423–415.
6. Froesch, E. R., Wolf, H. P., Baitsch, H., Prader, A., and Labhart, A. (1963) Hereditary fructose intolerance. An inborn defect of hepatic fructose-1-phosphate splitting aldolase. *Am. J. Med. 34*, 151–167.
7. Gaby, A. R. (2005) Adverse effects of dietary fructose. *Altern. Med. Rev. 10*, 294–306.
8. Coffee, E. M., Yerkes, L., Ewen, E. P., Zee, T., and Tolan, D. R. (2009) Increased prevalence of mutant null alleles that cause hereditary fructose intolerance in the American population. *J. Inherited Metab. Dis. 33*, 33–42.
9. Malay, A. D., Allen, K. N., and Tolan, D. R. (2005) Structure of the thermolabile mutant aldolase B, A149P: Molecular basis of hereditary fructose intolerance. *J. Mol. Biol. 347*, 135–144.
10. Malay, A. D., Procious, S. L., and Tolan, D. R. (2002) The temperature dependence of activity and structure for the most prevalent mutant aldolase B associated with hereditary fructose intolerance. *Arch. Biochem. Biophys. 408*, 295–304.
11. Beernink, P. T., and Tolan, D. R. (1996) Disruption of the aldolase A tetramer into catalytically active monomers. *Proc. Natl. Acad. Sci. U.S.A. 93*, 5374–5379.
12. Bolen, D. W., and Baskakov, I. V. (2001) The osmophobic effect: Natural selection of a thermodynamic force in protein folding. *J. Mol. Biol. 310*, 955–963.
13. Yancey, P. H., Clark, M. E., Hand, S. C., Bowlus, R. D., and Somero, G. N. (1982) Living with water stress: Evolution of osmolyte systems. *Science 217*, 1214–1222.
14. Yancey, P. H., Blake, W. R., and Conley, J. (2002) Unusual organic osmolytes in deep-sea animals: Adaptations to hydrostatic pressure and other perturbants. *Comp. Biochem. Physiol. 133*, 667–676.
15. Wang, A., and Bolen, D. W. (1997) A naturally occurring protective system in urea-rich cells: Mechanism of osmolyte protection of proteins against urea denaturation. *Biochemistry 36*, 9101–9108.
16. Gillett, M. B., Suko, J. R., Santoso, F. O., and Yancey, P. H. (1997) Elevated levels of trimethylamine oxide in muscles of deep-sea gadiform teleosts: A high-pressure adaptation? *J. Exp. Zool. 279*, 386–391.
17. Burg, M. B., and Ferraris, J. D. (2008) Intracellular organic osmolytes: Function and regulation. *J. Biol. Chem. 283*, 7309–7313.
18. Burg, M. B., Kwon, E. D., and Peters, E. M. (1996) Glycerophosphorylcholine and betaine counteract the effect of urea on pyruvate kinase. *Kidney Int. 50*, S100–S104.
19. Street, T. O., Bolen, D. W., and Rose, G. D. (2006) A molecular mechanism for osmolyte-induced protein stability. *Proc. Natl. Acad. Sci. U.S.A. 103*, 13997–14002.
20. Schellman, J. A. (2003) Protein stability in mixed solvents: A balance of contact interaction and excluded volume. *Biophys. J. 85*, 108–125.
21. Auton, M., Ferreon, A. C., and Bolen, D. W. (2006) Metrics that differentiate the origins of osmolyte effects on protein stability: A test of the surface tension proposal. *J. Mol. Biol. 361*, 983–992.
22. Minton, A. P. (1997) Influence of excluded volume upon macromolecular structure and associations in 'crowded' media. *Curr. Opin. Biotechnol. 8*, 65–69.
23. Saunders, A. J., Davis-Searles, P. R., Allen, D. L., Pielak, G. J., and Erie, D. A. (2000) Osmolyte-induced changes in protein conformational equilibria. *Biopolymers 53*, 293–307.
24. Davis-Searles, P. R., Saunders, A. J., Erie, D. A., Winzor, D. J., and Pielak, G. J. (2001) Interpreting the effects of small uncharged solutes on protein-folding equilibria. *Annu. Rev. Biophys. Biomol. Struct. 30*, 271–306.
25. Ralston, G. B. (1990) Effects of "crowding" in protein solutions. *J. Chem. Educ. 67*, 857–860.

26. Doyle, S. A., and Tolan, D. R. (1995) Characterization of recombinant human aldolase B and purification by metal chelate chromatography. *Biochem. Biophys. Res. Commun. 206*, 902–908.
27. Bradford, M. M. (1976) A rapid and sensitive method for the quantitation of microgram quantities of protein utilizing the principle of protein-dye binding. *Anal. Biochem. 72*, 248–254.
28. Eagles, P. A., and Iqbal, M. (1973) A comparative study of aldolase from human muscle and liver. *Biochem. J. 133*, 429–439.
29. Morris, A. J., and Tolan, D. R. (1993) Site-directed mutagenesis identifies aspartate 33 as a previously unidentified critical residue in the catalytic mechanism of rabbit aldolase A. *J. Biol. Chem. 268*, 1095–1100.
30. Racker, E. (1947) Spectrophotometric measurement of hexokinase and phosphohexokinase activity. *J. Biol. Chem. 167*, 843–854.
31. Brooks, B. R., Brooks, C. L., III, Mackerell, A. D., Nilsson, L., Petrella, R. J., Roux, B., Won, Y., Archontis, G., Bartels, C., Boresch, S., Caflisch, A., Caves, L., Cui, Q., Dinner, A. R., Feig, M., Fischer, S., Gao, J., Hodoscek, M., Im, W., Kuczera, K., Lazaridis, T., Ma, J., Ovchinnikov, V., Paci, E., Pastor, R. W., Post, C. B., Pu, J. Z., Schaefer, M., Tidor, B., Venable, R. M., Woodcock, H. L., Wu, X., Yang, W. D., York, M., and Karplus, M. (1998) CHARMM: The Biomolecular simulation Program. *J. Comput. Chem. 30*, 1545–1615.
32. Stanton, D. T., and Jurs, P. C. (1992) Computer-assisted study of the relationship between molecular structure and surface tension of organic compounds. *J. Chem. Inf. Comput. Sci. 32*, 109–115.
33. Bolen, D. W. (2004) Effects of naturally occurring osmolytes on protein stability and solubility: Issues important in protein crystallization. *Methods 34*, 312–322.
34. Beernink, P. T., and Tolan, D. R. (1994) Subunit interface mutants of rabbit muscle aldolase form active dimers. *Protein Sci. 3*, 1383–1391.
35. Choi, K. H., Lai, V., Foster, C. E., Morris, A. J., Tolan, D. R., and Allen, K. N. (2006) New superfamily members identified for Schiff-base enzymes based on verification of catalytically essential residues. *Biochemistry 45*, 8546–8555.
36. Morris, A. J., and Tolan, D. R. (1994) Lysine-146 of rabbit muscle aldolase is essential for cleavage and condensation of the C3-C4 bond of fructose 1,6-bis(phosphate). *Biochemistry 33*, 12291–12297.
37. Choi, K. H., Shi, J., Hopkins, C. E., Tolan, D. R., and Allen, K. N. (2001) Snapshots of catalysis: The structure of fructose-1,6-(bis)-phosphate aldolase covalently bound to the substrate dihydroxyacetone phosphate. *Biochemistry 40*, 13868–13875.
38. Zhang, Y. L., Zhou, J. M., and Tsou, C. L. (1993) Inactivation precedes conformation change during thermal denaturation of adenylate kinase. *Biochim. Biophys. Acta 1164*, 61–67.
39. Tsou, C. L. (1993) Conformational flexibility of enzyme active sites. *Science 262*, 380–381.
40. Patel, C. N., Noble, S. M., Weatherly, G. T., Tripathy, A., Winzor, D. J., and Pielak, G. J. (2002) Effects of molecular crowding by saccharides on α-chymotrypsin dimerization. *Protein Sci. 11*, 997–1003.
41. Bolen, D. W., and Rose, G. D. (2008) Structure and energetics of the hydrogen-bonded backbone in protein folding. *Annu. Rev. Biochem. 77*, 339–362.
42. Auton, M., and Bolen, D. W. (2004) Additive transfer free energies of the peptide backbone unit that are independent of the model compound and the choice of concentration scale. *Biochemistry 43*, 1329–1342.
43. Auton, M., and Bolen, D. W. (2005) Predicting the energetics of osmolyte-induced protein folding/unfolding. *Proc. Natl. Acad. Sci. U.S.A. 102*, 15065–15068.
44. Liu, Y., and Bolen, D. W. (1995) The peptide backbone plays a dominant role in protein stabilization by naturally occurring osmolytes. *Biochemistry 34*, 12884–12891.
45. Malay, A. D. (2004) The Structure and Function of the Most Prevalent Mutant Form of Aldolase B Associated with Hereditary Fructose Intolerance. Ph.D. Thesis, Boston University, Boston.
46. Fenton, A. W., Johnson, T. A., and Holyoak, T. (2010) The pyruvate kinase model system, a cautionary tale for the use of osmolyte perturbations to support conformational equilibria in allostery. *Protein Sci. 19*, 1796–1800.